Fusion Engineering and Design 84 (2009) 1125–1129

Contents lists available at ScienceDirect

Fusion Engineering and Design

journal homepage: www.elsevier.com/locate/fusengdes

Physics design requirements for the National Spherical Torus Experiment liquid lithium divertor

H.W. Kugel [a,*], M. Bell [a], L. Berzak [a], A. Brooks [a], R. Ellis [a], S. Gerhardt [a], H. Harjes [b], R. Kaita [a], J. Kallman [a], R. Maingi [b], R. Majeski [a], D. Mansfield [a], J. Menard [a], R.E. Nygren [c], V. Soukhanovskii [d], D. Stotler [a], P. Wakeland [e], L.E. Zakharov [a]

[a] *Princeton Plasma Physics Laboratory, P. O. Box 451, Princeton NJ NJ08543, USA*
[b] *Oak Ridge National Laboratory, Oak Ridge, TN, USA*
[c] *Sandia National Laboratories, Albuquerque, NM, USA*
[d] *Lawrence Livermore National Laboratory, Livermore, CA, USA*
[e] *K-Tech Corp., Albuquerque, NM, USA*

ARTICLE INFO

Article history:
Available online 22 January 2009

Keywords:
Lithium
Divertors
Lithium wall fusion regime

ABSTRACT

Recent National Spherical Tokamak Experiment (NSTX) high-power divertor experiments have shown significant and recurring benefits of *solid* lithium coatings on plasma facing components (PFCs) to the performance of divertor plasmas in both L- and H-mode confinement regimes heated by high-power neutral beams. The next step in this work is installation of a *liquid* lithium divertor (LLD) to achieve density control for inductionless current drive capability (e.g., about a 15–25% n_e decrease from present highest non-inductionless fraction discharges which often evolve toward the density limit, $n_e/n_{GW} \sim 1$), to enable n_e scan capability ($\times 2$) in the H-mode, to test the ability to operate at significantly lower density (e.g., $n_e/n_{GW} = 0.25$), for future reactor designs based on the Spherical Tokamak, and eventually to investigate high heat-flux power handling (10 MW/m^2) with long pulse discharges (>1.5 s). The first step (LLD-1) physics design encompasses the desired plasma requirements, the experimental capabilities and conditions, power handling, radial location, pumping capability, operating temperature, lithium filling, MHD forces, and diagnostics for control and characterization.

1. Introduction

Liquid lithium deposited on plasma-facing components (PFCs) shows promise for removing incident tritium and controlling impurities, providing a self-healing plasma facing surface in a diverted high-power DT reactor [1–3], and enabling a lithium wall fusion regime [4]. National Spherical Torus Experiment (NSTX) research with *solid* lithium is aimed initially toward using *liquid lithium* to control density, edge collisionality, impurity influxes, Edge Localized Mode (ELM) reduction and elimination, and eventually power handling. In current NSTX research on sustained non-inductive current drive in H-mode plasmas, lithium has the potential for control of secular density (n_e) rises, due to its ability to pump the atomic and ionic deuterium efflux by the formation of lithium deuteride. This formation of lithium deuteride effectively sequesters deuterium, thereby making it unavailable for recycling. Solid lithium does provide short pulse pumping capability, but the formation of lithium deuteride can saturate in the near surface layer (~250 μm) [5]. Liquid lithium has much higher lithium deuteride capacity [6], and has potential for reactor applications [1–4]. Over the longer term, NSTX will investigate if liquid lithium can help integrate four important potential benefits for fusion, (a) divertor pumping over large surface area compatible with high flux expansion solutions for power exhaust and low collisionality, (b) improved confinement [7,8], (c) reduction and elimination of ELMs [7–9], and (d) high-heat-flux handling. Motivated by the long range potential of lithium PFCs, NSTX has been investigating lithium pellet injection and lithium evaporation for density control and impurity control as part of a phased, three-part approach to lithium PFCs: first (i) lithium pellet injection [10], then (ii) lithium evaporators [7–9], and finally (iii) a liquid lithium divertor. This gradual approach is allowing NSTX control systems, diagnostics, and research to be adapted to the lithium wall fusion regime. NSTX has completed the first two parts of this program, and is moving aggressively toward the third phase, the liquid lithium divertor (LLD). The first step in the LLD program (LLD-1) is a design that uses lithium evaporated on thin porous molybdenum, vacuum flame-sprayed on a thin stainless-steel liner, brazed to a copper base-plate. The next step (LLD-2) may use capillary flow of lithium contained in a molybdenum mesh or foam layer to load a wider divertor area from a higher capacity reservoir near

* Corresponding author. Tel.: +1 609 243 3146; fax: +1 609 243 3248.
E-mail address: hkugel@pppl.gov (H.W. Kugel).

0920-3796/$ – see front matter © 2008 Elsevier B.V. All rights reserved.
doi:10.1016/j.fusengdes.2008.11.102

the divertor. This would enable n_e scan capability in long pulse H-mode (e.g., approx.×2) by varying lithium thickness and fueling. Testing the ability for sustained operation at significantly lower density ($n_e/n_{GW} \sim 0.25$–0.5) is of interest for the design of next step devices requiring bootstrap current drive (e.g., a fusion Component Test Facility (CTF) based on the Spherical Tokamak (ST)). The last step (LLD-3) will be designed for long pulse (5 s) power handling with a capillary fed surface and active cooling (e.g., capillary flowing lithium, high flow tubes, hypervaportrons, or evaporative cooling) for 16 MW high-power (10 MW NBI + 6 MW RF) operation. Installation of the LLD-1 is in progress. This paper describes the LLD-1 design that addresses the desired plasma performance, and experimental program requirements.

2. Experiment description

The parameters achievable on NSTX include $R_0 \leq 0.85$ m, $a \leq 0.67$ m, $R/a \geq 1.26$, $\kappa \leq 2.7$, $\delta \leq 0.8$, $I_p \leq 1.5$ MA, $B_T \leq 0.55$ T, and 1.5 s maximum pulse length [11]. Copper passive stabilizer plates, graphite power handling surfaces, 6 MW of deuterium Neutral Beam Injection (NBI) heating, 6 MW of 30 MHz High Harmonic Fast Wave (HHFW) for rf heating and current drive provide additional experimental versatility. The 0.2 m radius center stack (CS) is clad with alternating vertical columns of 1.3 cm thick graphite (Union Carbide, Type ATJ) tiles between columns of 2-D Carbon Fiber Composite (Allied Signal, Type 865-19-4) tiles. The inner divertor tiles are 5.1 cm thick Type ATJ graphite; the outer divertor and passive stabilizer plate tiles are 2.5 cm thick Type ATJ graphite. The PFCs are conditioned as required using vacuum bakeout at 350 °C, Helium Glow Discharge Cleaning (HeGDC) between discharges, and boronization. A sabot-style Lithium Pellet Injector (LPI) can inject lithium, other low-Z pellets, or powders into edge plasmas. The NSTX configuration enables experiments with ohmic, NBI, and HHFW rf heating in CS limiter start-up, lower single-null diverted (LSND), and double-null diverted (DND) discharges, with Coaxial Helicity Injection (CHI).

Fig. 1 shows a schematic diagram of the poloidal cross section of NSTX, the locations of the two lithium evaporators (LITERs) at toroidal angles 165° and 315°, and the LITER central-axis aimed at the lower divertor, with dashed lines indicating the gaussian half-angles at $1/e$ intensity of the measured evaporated Li angular distributions. Fig. 2 shows a schematic of the LLD-1 installed near the inner edge of the outer divertor. It will consist of four 90° sections, each 20 cm wide in the radial direction. The plasma facing surface is a thin porous layer of 0.010 cm molybdenum, flame-sprayed on a 0.025 cm stainless steel liner, brazed to a 2.222 cm copper baseplate. Resistive heaters and cooling lines maintain a temperature range from room temperature to 400 °C. A row of ATJ diagnostic tiles separates each 90° LLD-1 segment. The diagnostic tiles contain 2-D magnetic sensors, Langmuir Probes, edge biasing electrodes, and thermocouples. The LITER evaporators (Fig. 1) will be used initially to load LLD-1. Additional information on the engineering design and thermal control of LLD-1 is given in a companion paper [12].

3. Physics design

The NSTX LLD-1 physics design encompasses both the desired plasma physics requirements, and the experimental capabilities and conditions for achieving them.

3.1. NSTX LLD-1 physics plasma requirements

In the present experiments, the highest non-inductive fraction discharges presently often evolve toward the density limit

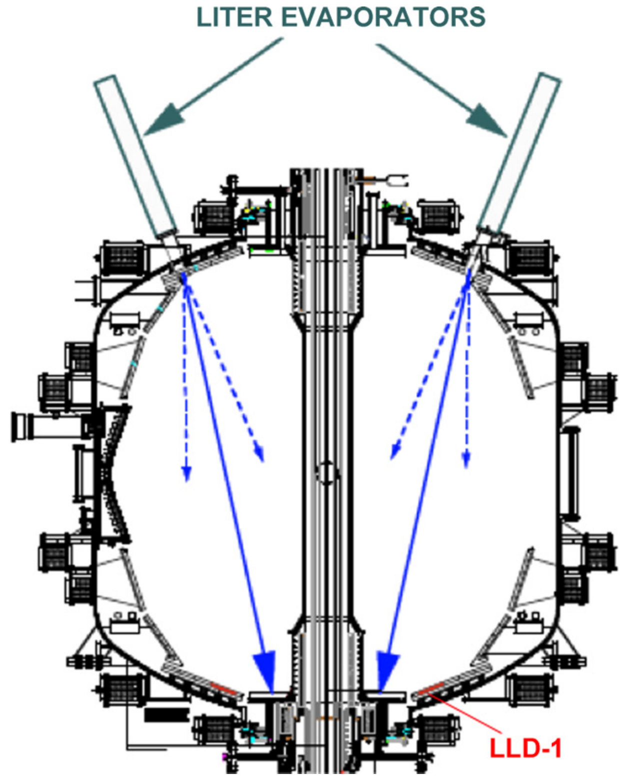

Fig. 1. Schematic diagram of the poloidal cross section of NSTX, the locations of the two lithium evaporators (LITERs) at toroidal angles 165° and 315°, and the LITER central-axis aimed at the lower divertor, and dashed lines indicating the Gaussian half-angles at $1/e$ intensity of the measured evaporated Li angular distributions.

($n_e/n_{GW} \sim 1$). The goal of the LLD-1design is to achieve density (n_e) reductions in the range of 25–50% which are predicted to increase NSTX neutral beam current drive efficiency and enable access to high (∼100%) non-inductive current fractions for plasmas with operating currents in the range of 700–800 kA [13].

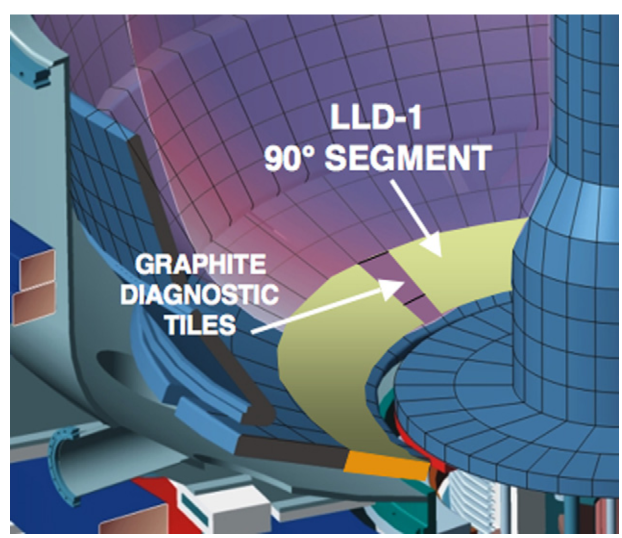

Fig. 2. Schematic of the LLD-1 installed near the inner edge of the outer divertor. It will consist of four 90° sections, each 20 cm wide in the radial direction. The plasma facing surface is a thin porous layer of 0.010 cm molybdenum flame-sprayed on 0.025 cm stainless steel liner, brazed to a 2.222 cm copper baseplate. Resistive heaters and cooling lines maintain a temperature range of 200–400 °C.

3.2. Experimental physics capability requirements

3.2.1. Power handling

The power handling ability of LLD-1 is important for vessel protection during the initial testing, and allowing a sufficient range of input powers for characterization of future designs. Extensive initial modeling of various candidate LLD-1 lithium surfaces configurations was performed (http://w3.pppl.gov/∼zakharov/). Based on these initial results, and additional engineering analysis [12], the first tests of the LLD-1 design limits power handling to low power (1.5 MW), short pulse (500 ms) deuterium NBI discharges to minimize lithium front face temperature rises above 400 °C. Higher powers and longer discharge durations may be tested by sweeping the outer strike-point over the LLD-1 to minimize local heat transfer [12].

3.2.2. Radial location

An important physics program issue addressed in the specification of the radial location was to minimize impact to the planned NSTX experimental research campaign, if the initial LLD-1 installation encountered a malfunction, or any operational difficulties during the early stages of testing. Since most NSTX, low aspect ratio (*R/a*), high elongation, high triangularity discharges have divertor strike-points on the inner divertor close to the center stack, the placement of LLD-1 farther out on the outer divertor was adopted, as the initial lowest risk location for extended experimental research campaigns involving a range of plasma conditions.

In addition, there is a secondary technical issue involving LLD-1 radial location that minimizes experimental physics operating risk. In particular, the LLD-1 outer divertor location avoids perturbing, or reinstalling, the complex inner divertor region with its high density of well-characterized magnetic sensors used for plasma control.

The outer divertor location is sloped 21.5° downward toward the inner divertor and CHI gap. Preliminary NSTX laboratory tests indicate that for the initial LLD-1 lithium thicknesses that will be deposited (2–20 μm) capillary forces from the vacuum flame-sprayed molybdenum plasma facing surface will be sufficient to overcome gravitational induced flow over the lower edge.

3.2.3. Pumping capability

Preliminary estimates of LLD-1 pumping projections and sensitivities were performed for the outer divertor location and various widths using a 0-D model. The calculations were parameterized as a ratio of pump to core fueling probabilities, and an initial incident deuterium sticking probability of 0.85. The pumping efficiency was obtained as a ratio of the integral of the incident flux over LLD-1 to the incident flux over the entire divertor. Actual NSTX discharges were used to obtain the radial dependence of the flux for various discharge shapes, the inner-to-outer strike point ratios, and the up/down particle flux ratios. Fig. 3 shows equilibrium flux plots for two different discharges incident on a 20 cm wide LLD-1 located on the outer divertor. The 0-D pumping simulation gives an estimated 50% density reduction for a low triangularity discharge with an outer strike point on LLD-1 (Fig. 3a). The same simulation gives an estimated 25% density reduction for a high triangularity discharge with the outer strike point located on the inner edge of the inner divertor (Fig. 3b) due to the high flux expansion between the midplane and the divertor (e.g., ×15–20). These results indicate that a 20 cm wide LLD-1 on the inner edge of the outboard divertor should provide sufficient density reduction to accommodate the physics plasma requirements (cf. Section 3.1). The actual density reduction factor will depend strongly on how quickly core fueling efficiency increases with decreasing density. Detailed comparisons of the 0-D model with UEDGE calculations are in progress.

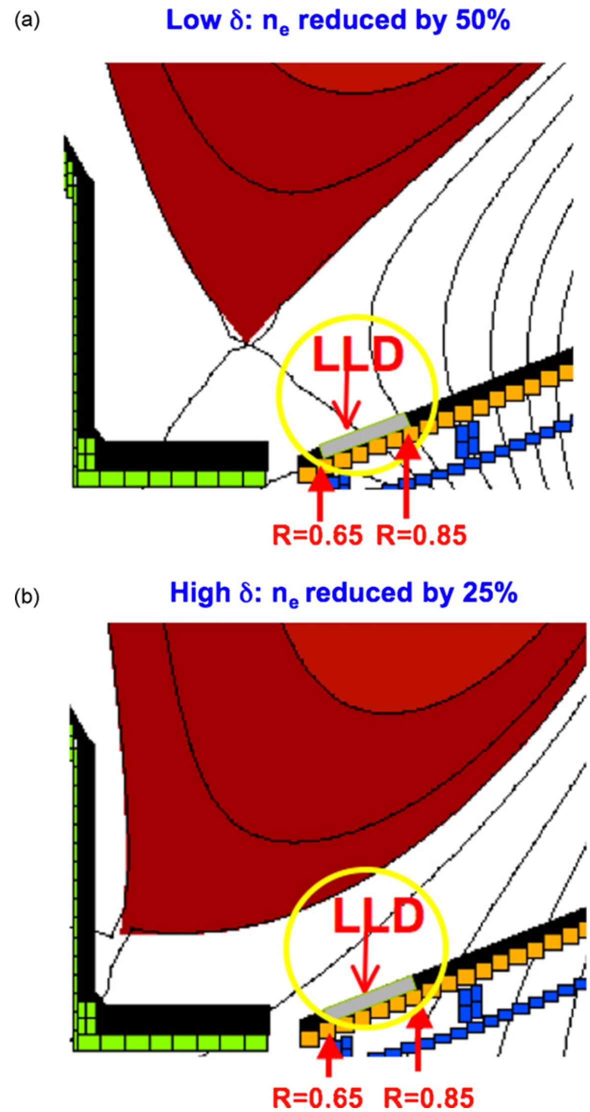

Fig. 3. Shown are equilibrium flux plots for two different discharges incident on a 20 cm wide LLD-1 located on the outer divertor. The 0-D pumping simulation gives an estimated 50% density reduction for a low triangularity discharge with an outer strike point on LLD-1 (a). The same simulation gives an estimated 25% density reduction for a high triangularity discharge with the outer strike point located on the inner edge of the inner divertor (b) due to the high flux expansion between the midplane and the divertor (e.g., × 15–20).

3.2.4. Operating temperature

Fig. 4 shows the lithium evaporation rate (mg/min) from the LLD-1 surface *versus* temperature. The nominal LLD-1 initial temperature range prior to a discharge will be in the range from ambient temperature to 400 °C. Prior to each discharge, the LLD-1 design allows the initial temperature to be selected for the desired experimental conditions, and then established by resistive heating and/or helium gas cooling of the copper substrate. In the case of discharges starting from liquid lithium conditions, the initial operating temperature range will be from slightly above the melting point of 180.5 °C to below 400 °C. This will minimize surface evaporation from its 2.3×10^3 cm^2 plasma facing surface area, and avoid the high temperature liquid lithium regime (>450 °C) where the decomposition of LiD results in the subsequent emission of deuterium [6].

3.2.5. Lithium-filling

The lithium loading and replenishment of LLD-1 needs to be done under vacuum conditions. LLD-1 for the initial experiments

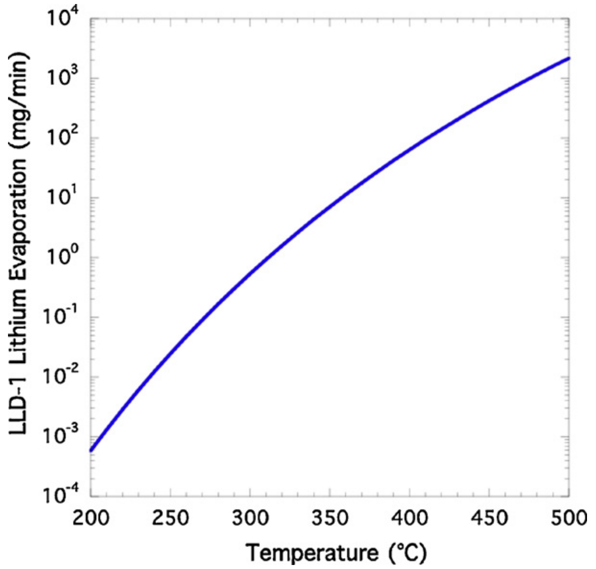

Fig. 4. The lithium evaporation rate (mg/min) from the LLD-1 surface *versus* temperature.

will be loaded with lithium using the existing dual LITERs aimed as shown in Fig. 1. Shown in Fig. 5 is a simulation of the lithium deposition [14] over the lower divertor region and the LLD-1. A typical NSTX deuterium discharge contains 2.4×10^{20} deuterium particles. If the LLD-1 were required to pump all deuterium efflux from the plasma, over every particle confinement time (assume conservatively ~50 ms), for a discharge of length 1000 ms, then a total of 4.8×10^{21} deuterium particles would be absorbed. Laboratory experiments have shown that ionic and atomic deuterium can be absorbed to a stoichiometric ratio of 1 (i.e., 1:1 Li/D), and that the resultant LiD has a saturation limit of 10% in liquid lithium [6]. If the LLD-1 absorbed deuterium atoms until this ratio is reached, this would consume 5.5×10^{-2} g of lithium (2 μm thickness on LLD-1). The present LITER deposition efficiency on to LLD is ~7% of it total output, and hence, the total lithium need is 0.79 g. Using 2 LITER

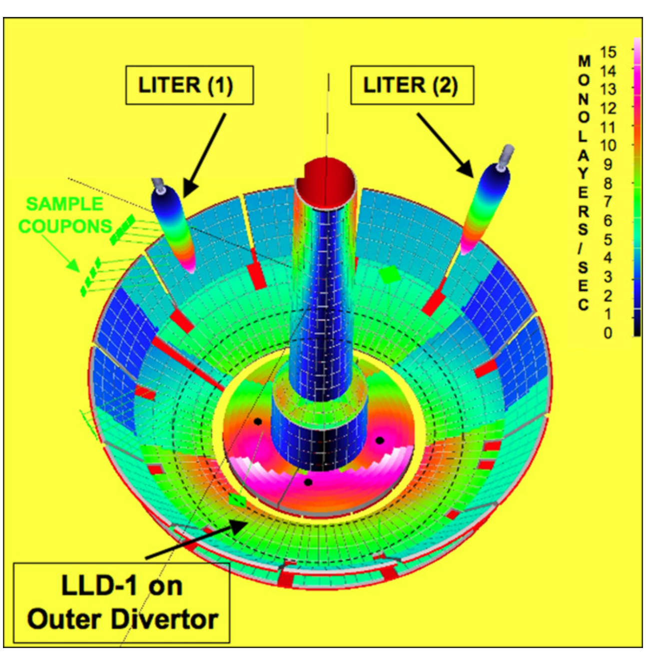

Fig. 5. Simulated lithium deposition shown on a partial schematic diagram of the NSTX lower divertor region and the LLD-1.

evaporators (Fig. 1) at 30 mg/min (typical LITER evaporation rates) will require about 13 min to coat the LLD-1. This is comparable to the time between NSTX discharges, and comparable to typical LITER deposition times used previously [8]. If for some experiments, a lower D/Li concentration ratio of 0.1 is tested, this would require 7.9 g of lithium (20 μm thickness on LLD-1), or 4 g per LITER, operating at 100 mg/min for 40 min. This is an acceptable deposition time for special tests.

3.2.6. MHD forces and the number of segments

The LLD-1 design requirements for experimental physics operation must accommodate the effects of induced halo currents from plasma current (I_p) disruptions and other off-normal MHD events. While the copper baseplate of LLD-1 requires at least 1 toroidal break to interrupt induced toroidal current flows, additional segmenting of LLD-1 has installation, maintenance, and diagnostic instrumentation advantages. Actual discharge data and simulations were used to determine that an LLD-1 designed in four segments is optimal for NSTX installation, and can accommodate the estimated induced forces. In particular, disrupted plasma current quench rates up to 1 GA/s have been measured in NSTX, and maximum instantaneous quench rates can significantly exceed average quench rates. The field variation at the inboard edge of the outer divertor is faster than any other location on the outboard divertor, due to its proximity to the X-point of diverted plasmas. The field variation time-scale is set by both the I_p quench rate and the plasma position evolution, which includes vertical motion. These observations indicate that at the LLD-1 outer divertor location, an average field time-derivative during I_p quench of up to 25 T/s for the normal field, and 200 T/s for the tangent field, and even larger instantaneous rates of change need to be accommodated in the LLD-1 design. Simulations indicate that the vertical force (F_z) on each LLD-1 curved edge is ~1.25 kN and F_z on each straight edge is ~2.18 kN. Each LLD-1 segment is supported at each of its four corners [12] to accommodate these forces, as well as, allow for thermal expansion, and electrical isolation. Electrical contact to the NSTX divertor structure is performed at one center grounding point so as to channel all induced halo currents through this point, and eliminate induced current loops. In addition, the installation of a Rogowski coil around this grounding point on each segment allows for characterizing these halo currents which will be essential data for the design of future embodiments of the LLD.

3.2.7. Diagnostics for control and characterization

The LLD-1 design requirements for experimental physics operation include the special diagnostics for controlling, and monitoring LLD-1 operation, and a thorough characterization for the design of future embodiments. Each 90° segment of LLD-1 has 12 thermocouples embedded in each of the 12 heaters [12] for monitoring heater limits, 12 thermocouples embedded in copper baseplate for monitoring heat transfer, 2 strips of 4 thermocouples each for torodial and radial temperature variations, and 1 center post halo current Rogowski coil for monitoring induced currents. In addition, each set of the 4 inter-segment graphite tiles has diagnostic sensors. Set-1 contains the existing 2-D magnetic sensor array presently used for control and equilibrium analysis, and thermocouples for IR camera calibrations. Set-2 contains a 120 elements Langmuir Probe array for single and triple probe measurements. Set-3 has 2 biased electrodes for edge biasing studies, 5 Langmuir Probes, and a thermocouple. Set-4, at toroidally 180° opposite this location, has the same configuration, i.e., 2 biased electrodes for edge biasing studies, 5 Langmuir Probes, and a thermocouple.

The design requirements for experimental physics operation specify special external diagnostics. A slow IR camera (33 Hz) will monitor slow changes in thermal conditions before, during and after discharges. A Fast IR camera (20 kHz) will be used to measure power deposition during ELMs and off-normal events. Since the IR emissivity of the bright liquid lithium surface may be changed as the lithium absorbs increasing amounts of fuel gas and residual components of the vacuum partial pressure (H_2O, D_2O, CO, CO_2), IR camera calibration for absolute measurements may be challenging. Thermocouples under LLD-1 and in the inter-segment graphite diagnostic tiles will facilitate recalibration under changing conditions. In addition, 2-color IR camera measurements will be investigated to allow absolute measurements, independent of lithium surface emissivity. Reflections from the bright liquid lithium surface and lithium on vessel structures will interfere with recycling measurements based on visible luminosity. This will be addressed by installing a Lyman-α Diode Array for recycling measurements at the LLD-1, since the reflectivity of liquid lithium is far less at this wavelength. The LLD-1 lithium thickness and reflectivity will be monitored using a LASER reflectometer.

4. Discussion and conclusions

The NSTX LLD-1 physics design encompasses both the desired plasma requirements, and the experimental capabilities and conditions for operating in this regime. Extensive analysis indicates that for comparable pumping speeds, the lowest risk location for LLD-1 to high performance, low aspect ratio (R/a) discharges is the outer divertor. LLD-1 with a 20 cm width pumping on outer divertor will provide reduction in density for both high performance discharges and inductionless current drive experiments. LLD-1 operation will be restricted to below 400 °C to avoid excessive lithium evaporation and disassociation, and emission of deuterium bound in LiD. The LLD-1 located on the outer divertor allows easiest access to feed-thrus and allows easiest modification of instrumentation. The existing dual unit LITER lithium evaporation system will be used for the initial lithium fill and replenishment. Later embodiments may use a capillary flow system. NSTX LLD-1 is the first step toward testing the potential benefits of liquid lithium divertor with high power ST plasmas in the lithium wall fusion regime [4], and over the longer term, investigating if liquid lithium can help demonstrate its promising potential benefits for fusion.

Acknowledgments

This work is supported by United States Department of Energy (US DOE) Contracts DE-AC02-76CH03073 (PPPL), DE-AC05-00OR22725 (ORNL), and those of Lawrence Livermore National Laboratory in part under Contract W-7405-Eng-48 and in part under Contract DE-AC52-07NA27344, and that of Sandia, a multi-program laboratory operated by Lockheed Martin Company, for the United States Department of Energy's National Nuclear Security Administration, under contract DE-AC04-94AL85000.

References

[1] Fus. Eng. Design 72 1-326 (2004). A large section of the "Special Issue on Innovative High-Power Density Concepts for Fusion Plasma Chambers" highlighted progress in this effort, and it continues as a primary focus of the "Advanced Limiter/Divertor Plasma-Facing Components (ALPS) DOE program.
[2] V.A. Evtikhin, I.E. Lyublinski, A.V. Vertkov, S.V. Mirnov, V.B. Lazarev, N.P. Petrova, et al., Plasma Phys. Control Fusion 44 (2002) 955, and references therein.
[3] S.V. Mirnov, In Proc. 18th International Conference on Plasma Surface Interactions, May 26–30, Toledo, Spain, 2008.
[4] L.E. Zakharov, N.N. Gorelenkov, R.B. White, S.I. Krasheninnikov, G.V. Pereverzev, Fus. Eng. Design 72 (2004) 149.
[5] J.N. Brooks, N. Brooks, J.P. Allain, T.D. Rognlien, R. Maingi, J. Nucl. Mater. 337–339 (2005) 1053.
[6] M.J. Baldwin, M.J. Baldwin, R.P. Doerner, S.C. Luckhardt, R.W. Conn, Nucl. Fusion 42 (2002) 1318.
[7] H.W. Kugel, M.G. Bell, J.-W. Ahn, J.P. Allain, R. Bell, J. Boedo, et al., Phys. Plasmas 15 (2008) 056118.
[8] H.W. Kugel, D. Mansfield, R. Maingi, M.G. Bell, R.E. Bell, J.P. Allain, et al., In Proc. 18th International Conference on Plasma Surface Interactions, May 26–30, Toledo, Spain, 2008.
[9] D.K. Mansfield, H.W. Kugel, R. Maingi, M.G. Bell, R. Bell, R. Kaita, et al., In Proc. 18th International Conference on Plasma Surface Interactions, May 26–30, Toledo, Spain, 2008.
[10] H.W. Kugel, M.G. Bell, R. Bell, C. Bush, D. Gates, T. Gray, et al., J. Nucl. Mater. 363–365 (2007) 791.
[11] M.G. Bell, R.E. Bell, D.A. Gates, S.M. Kaye, H. Kugel, B.P. LeBlanc, et al., Nucl. Fusion 46 (8) (2006) S565, and references therein.
[12] R.E. Nygren, H.C. Harjes, P. Wakeland, R. Ellis, H.W. Kugel, R. Kaita, et al., in this issue.
[13] C.E. Kessel, R.E. Bell, M.G. Bell, D.A. Gates, S.M. Kaye, B.P. LeBlanc, Phys. Plasmas 13 (2006) 056108.
[14] L.E. Zakharov, H.W. Kugel, A.L. Roquemore, C.H. Skinner, Bull. Am. Phys. Soc. 52 (2007) 267.